

# Alkalinity production in intertidal sands intensified by lugworm bioirrigation



Alexandra M.F. Rao <sup>a,\*</sup>, Sairah Y. Malkin <sup>a,1</sup>, Francesc Montserrat <sup>a,b</sup>, Filip J.R. Meysman <sup>a,b</sup>

<sup>a</sup> Laboratory of Analytical, Environmental & Geochemistry, Vrije Universiteit Brussel, Pleinlaan 2, B-1050 Brussels, Belgium

<sup>b</sup> Department of Ecosystem Studies, Royal Netherlands Institute for Sea Research, P.O. Box 140, 4400 AC Yerseke, The Netherlands

## ARTICLE INFO

### Article history:

Received 16 September 2013

Accepted 5 June 2014

Available online 26 June 2014

### Keywords:

diagenesis

bioirrigation

bioturbation

*Arenicola*

calcium carbonate

alkalinity

## ABSTRACT

Porewater profiles and sediment-water fluxes of oxygen, nutrients, pH, calcium, alkalinity, and sulfide were measured in intertidal sandflat sediments from the Oosterschelde mesotidal lagoon (The Netherlands). The influence of bioturbation and bioirrigation by the deep-burrowing polychaete *Arenicola marina* on the rates and sources of benthic alkalinity generation was examined by comparing measurements in intact and defaunated sediment cores before and after the addition of *A. marina* in summer and fall 2011. Higher organic matter remineralization rates, shallower O<sub>2</sub> penetration, and greater sediment-water solute fluxes were observed in summer, consistent with higher sediment community metabolic rates at a higher temperature. Lugworm activity stimulated porewater exchange ( $5.1 \times$  in summer,  $1.9 \times$  in fall), organic matter remineralization ( $6.2 \times$  in summer,  $1.9 \times$  in fall), aerobic respiration ( $2.4 \times$  in summer,  $2.1 \times$  in fall), alkalinity release ( $4.7 \times$  in summer,  $4.0 \times$  in fall), nutrient regeneration, and iron cycling. The effects of lugworm activity on net sediment-water fluxes were similar but more pronounced in summer than in fall. Alkalinity release in fall was entirely driven by metabolic carbonate dissolution, while this process explained between 22 and 69% of total alkalinity production in summer, indicating the importance of other processes in this season. By enhancing organic matter remineralization and the reoxidation of reduced metabolites by the sediment microbial community, lugworm activity stimulated the production of dissolved inorganic carbon and metabolic acidity, which in turn enhanced metabolic CaCO<sub>3</sub> dissolution efficiency. In summer, evidence of microbial long distance electron transport (LDET) was observed in defaunated sediment. Thus, alkalinity production by net carbonate dissolution was likely supplemented by anaerobic respiration and LDET in summer.

© 2014 The Authors. Published by Elsevier Ltd. This is an open access article under the CC BY-NC-ND license (<http://creativecommons.org/licenses/by-nc-nd/3.0/>).

## 1. Introduction

Oceans are an important sink for the excess CO<sub>2</sub> released by human activities including fossil fuel burning, land use change, industrialization and deforestation, which have resulted in a >30% rise in atmospheric CO<sub>2</sub> during the industrial era (Sabine et al., 2004; Forster et al., 2007). In this time, the oceans have absorbed approximately 30% of anthropogenic CO<sub>2</sub> emissions by air-sea gas exchange, resulting in a decline in surface ocean pH of about 0.1 (Feely et al., 2010). In the last century, ocean acidification has had a significant negative effect on calcification, survival, growth, development, and abundance among corals, mollusks, echinoderms,

coccolithophores, and other taxonomic groups (Kroeker et al., 2013). With an additional expected decline of 0.3–0.4 pH by the end of this century, ocean uptake of anthropogenic CO<sub>2</sub> will likely have strong adverse effects on calcareous and noncalcareous marine organisms alike (Gazeau et al., 2007; Guinotte and Fabry, 2008; Hutchins et al., 2009).

In coastal waters, the accumulation of anthropogenic CO<sub>2</sub> can exacerbate low pH conditions resulting from natural respiration processes (Feely et al., 2008; Bates and Mathis, 2009; Feely et al., 2010), thereby compounding the stress exerted on coastal ecosystems. While sediments represent an important site of organic matter remineralization in nearshore environments, recent studies suggest that coastal sediments are also a source of alkalinity to the overlying water, favoring the role of the coastal ocean as a potential sink for atmospheric CO<sub>2</sub> (Thomas et al., 2009; Faber et al., 2012). During early diagenesis, alkalinity can be produced by several different processes, including CaCO<sub>3</sub> dissolution, denitrification, and iron and sulfate reduction coupled to the subsequent

\* Corresponding author. Present address: Université du Québec à Rimouski, Institut des sciences de la mer, 310 allée des Ursulines C.P. 3300, Rimouski QC, G5L 3A1 Canada.

E-mail address: [alexandra\\_rao@uqar.ca](mailto:alexandra_rao@uqar.ca) (A.M.F. Rao).

<sup>1</sup> Present address: Department of Marine Sciences, University of Georgia, Athens, GA, USA.

burial of iron sulfide minerals such as iron monosulfide (FeS) and pyrite (FeS<sub>2</sub>) (Stumm and Morgan, 1996). It is crucial to better understand the actual mechanisms and rates of benthic alkalinity generation.

In the North Sea, it has been estimated that as much as one-quarter of the overall CO<sub>2</sub> uptake may be driven by alkalinity production in the intertidal flats of the southern North Sea (Thomas et al., 2009). These deposits support rich macrofaunal communities (Reise et al., 1994; Seys et al., 1994) and high sediment community metabolic rates (de Beer et al., 2005; Werner et al., 2006; Roy et al., 2008). The macrofaunal activity in these sediments exerts an important influence on carbon and nutrient cycling and fluxes of solutes across the sediment–water interface by altering the balance between solute transport and reaction rates in sediments (Kristensen, 2001). An understanding of the influence of benthic macrofauna in regulating alkalinity production may therefore help to elucidate the rates, controls, and spatiotemporal variability in alkalinity sources and CO<sub>2</sub> uptake in ocean margin environments. Experimental and modeling studies have shown that biological particle mixing (bioturbation) exerts a strong control on the permeability, stability, composition, and metabolic rates in sediments, and that bioirrigation flushes out reduced metabolites and supplies terminal electron acceptors and organic substrates for microbial metabolism (Banta et al., 1999; Kristensen, 2001; Volkenborn et al., 2007; D'Andrea and DeWitt, 2009; Volkenborn et al., 2010; Kristensen et al., 2012). However, the influence of benthic macrofaunal activity on alkalinity generation has so far received little attention.

To better understand the role of macrofaunal activity (particle mixing and porewater bioirrigation) on alkalinity production in coastal sediments, we investigated the impact of the deep-burrowing lugworm *Arenicola marina* on interfacial fluxes and porewater profiles of oxygen, nutrients, pH, calcium, alkalinity, and sulfide in sediment cores from an intertidal sandflat in the Oosterschelde (The Netherlands). The effect of season was investigated by comparing experiments conducted in summer and in autumn.

*A. marina* is the dominant bioirrigator in intertidal sediments in the southern North Sea, and at densities that can exceed 50 individuals per m<sup>-2</sup>, it often dominates the polychaete biomass in this region (Reise et al., 1994; Coosen et al., 1994; Kristensen, 2001). The lugworm is a head-down deposit feeder residing in L-shaped burrows that can conspicuously transform its habitat (Huettel, 1990; Volkenborn et al., 2007). Sediment ingestion in the lower part of the burrow causes sediment to sink into the feeding pocket, and the resulting surface depression traps detritus. The lugworm periodically retreats to the surface and excretes sediment particles around the opening of the tail shaft, producing distinctive faecal casts. This ingestion–egestion behavior reworks the sediments surrounding the burrow structures, and translocates surface sediments with recently deposited labile organic material and solid phase electron acceptors, such as iron and manganese (hydr)oxides, downward into subsurface suboxic or anoxic layers of sediment. At the same time, aged, refractory organic particles and reduced iron sulfide minerals are transported upward to the oxic surface layer. The peristaltic motions of *A. marina* result in the irrigation of burrow water with oxygenated bottom water in a rhythmic fashion and the percolation of suboxic or anoxic porewater surrounding the feeding pocket upward into the overlying water, although flow reversals do occur (Kristensen, 2001; Volkenborn et al., 2010). The bioturbation and bioirrigation activities of lugworms enhance aerobic and anaerobic mineralization of organic carbon and nitrogen in sandy coastal sediments (Kristensen, 1988; Huettel, 1990; Banta et al., 1999; Kristensen, 2001).

## 2. Materials and methods

### 2.1. Sampling

Sediment cores were collected by hand at low tide at Tholseinde (51° 26' 52" N, 04° 05' 47" E, Fig. 1), an intertidal region in the inner part of the Oosterschelde (Delta area, SW Netherlands). The Oosterschelde is an euhaline mesotidal basin with extensive intertidal sandflats, which cover about one-third of its surface area (de Jong et al., 1994). Hydrodynamic forces and sediment transport in this coastal embayment have been modified by a storm-surge barrier and two auxiliary dams, completed in 1987 (ten Brinke et al., 1994; de Jong et al., 1994; Nienhuis and Smaal, 1994). The Oosterschelde sandflats are home to a rich macrofaunal community of bivalves, gastropods, and polychaetes, most notably the lugworm *Arenicola marina* (Coosen et al., 1994).

### 2.2. Core incubations

Sediment cores were collected in July and November 2011, and brought to the Royal Netherlands Institute for Sea Research (NIOZ) in Yerseke, NL for *ex situ* incubations. Plexiglas (PMMA) coreliners, 15 cm inner diameter and 35 cm in length, were used for collection and subsequent incubations. Cores typically contained about 20 cm of sediment and 15 cm of overlying water. Cores were incubated in a darkened water bath, continuously aerated and replaced daily with Oosterschelde seawater, kept in a temperature-controlled room at 16 °C in July and 12 °C in November.

In July, eight cores were collected and immediately sealed with polyoxymethylene lids with gas-tight O-ring seals after collection for a ten day period of defaunation by asphyxia. Cores were then opened and any macrofauna that had migrated to the surface were carefully removed with minimal disturbance to the sediment–water interface. The open cores were then placed in the aerated water bath for a reequilibration period of eight days. Subsequently, O<sub>2</sub>, pH and H<sub>2</sub>S microsensor profiles were measured in triplicate in each of three cores, as described in Section 2.4, and solute fluxes were determined in all eight cores as described in Section 2.3. Two adult *Arenicola* specimens were introduced in each core, and it was verified that the lugworms burrowed into the sediment. Two days after lugworm addition, flux measurements were repeated in all cores and microprofiles were measured in two cores, both in areas that appeared undisturbed by lugworm activity ( $n = 3$  replicate profiles of each solute per core) and in areas covered with *Arenicola* faecal casts ( $n = 2$  replicate profiles of each solute per core).

In November, ten cores were collected and brought into the laboratory for incubation. The incubation procedure was largely similar to the July experiment, but in addition to the measurements made in defaunated cores before and after lugworm addition, the initial conditions were also characterized in cores shortly after collection (hereafter referred to as “intact cores”). To this end, porewater O<sub>2</sub>, pH and H<sub>2</sub>S microprofiles ( $n = 5$  replicate profiles of each solute) were measured after one day of reequilibration in two intact cores, P1 and P2, which were dedicated for microprofile measurements throughout the entire experiment. After two days of reequilibration, solute flux measurements (Section 2.3) were made in cores P1, P2, and three additional intact cores. Two of these intact cores were then destructively sampled for solid phase and porewater analyses as described in Section 2.4. The remaining cores were sealed for a twenty-five day defaunation period, reopened and macrofauna that had surfaced were carefully removed. Cores were then kept open in the aerated water bath for a nine day reequilibration period. Subsequently, porewater O<sub>2</sub>, pH and H<sub>2</sub>S microprofiles ( $n = 3$  replicate profiles of each solute) were measured under defaunated conditions, and flux measurements

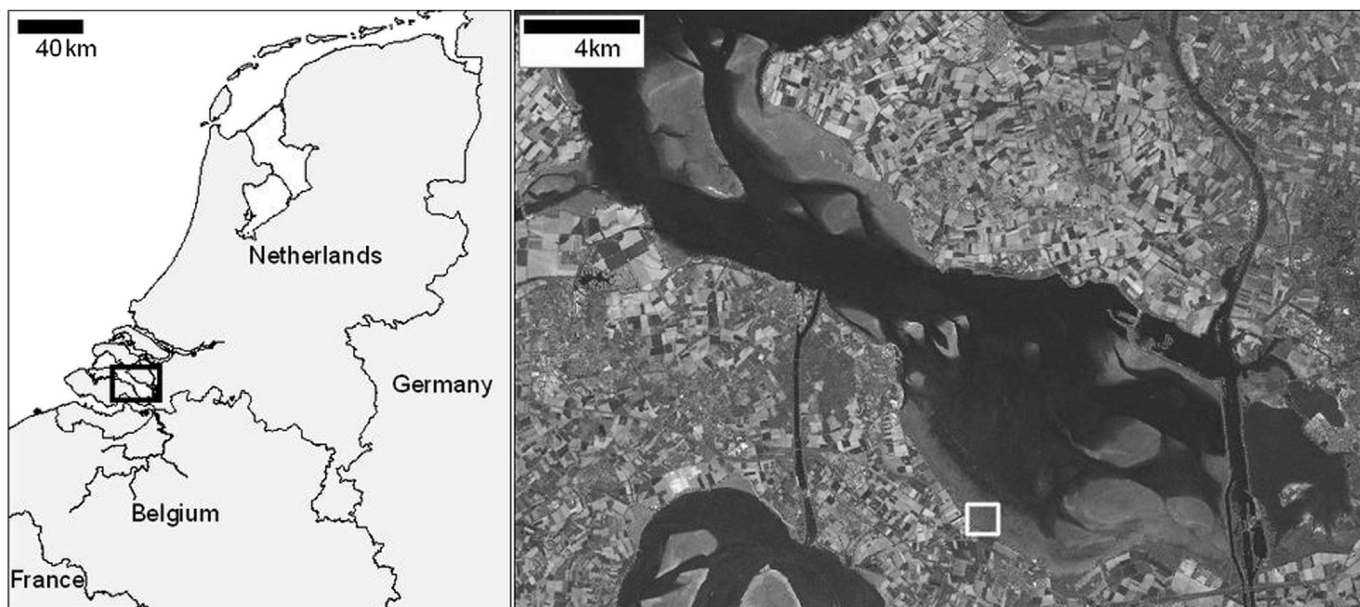


Fig. 1. The Oosterschelde embayment, with the location of the sampling site at Tholseinde marked with a square.

were made in cores P1, P2, and three additional cores, which were destructively sampled for solid phase and porewater analyses on the following day. Two adult *Arenicola* specimens were introduced in each of the five remaining cores. Five days after lugworm addition, porewater  $O_2$ , pH and  $H_2S$  microprofiles were measured, both in areas that appeared undisturbed by lugworm activity ( $n = 3$  replicate profiles of each solute per core) and in areas covered with *Arenicola* faecal casts ( $n = 2$  replicate profiles of each solute per core). The following day, flux measurements were conducted in cores P1, P2, and the remaining three cores, which were destructively sampled for solid phase and porewater analyses on the following day. In the following sections, we compare measurements in intact and defaunated cores before and after lugworm addition.

### 2.3. Solute flux measurements

Solute fluxes across the sediment–water interface were measured in closed core incubations. Each set of flux measurements was begun by securing gas-tight lids on each core in a water bath. Core lids contained two sampling ports on opposite sides and a central stirrer to ensure that the overlying water remained well mixed during incubation. Both ports were purged prior to the start of each incubation, to ensure that no gas bubbles remained. An oxygen optode (PreSens oxygen dipping probe or Pyrosience robust oxygen probe OXROB10) was inserted into a third opening in each lid and secured by a rubber stopper, for measurements of total oxygen uptake (TOU). Optodes were pre-calibrated on the same day using a two-point calibration with Oosterschelde seawater at 0% and 100%  $O_2$  saturation, bubbled with nitrogen gas and air, respectively. Oxygen data from one defaunated core in July were excluded from final analysis due to optode malfunction.

At the start of closed core incubations, a known volume of sodium bromide (NaBr) tracer solution was added to the overlying water of each core, to a final concentration of 3–5 mmol  $L^{-1}$ . The initial spike solution was prepared at concentrations between 0.2 and 0.3 mol  $L^{-1}$  NaBr, such that its density matched that of the overlying water at the start of incubations. Samples of about 30 mL of overlying water were collected from each core in plastic syringes approximately hourly for analysis of dissolved inorganic nutrients,

pH, total alkalinity (TA), calcium ( $Ca^{2+}$ ) and bromide ( $Br^-$ ), as described in Section 2.5.

The volume of overlying water and the rate of porewater exchange by bioirrigation were calculated from the dilution of  $Br^-$  tracer in the overlying water of each core. The effective overlying water volume ( $V_{ow}$ ) was determined from the known volume ( $V_{spike}$ ) and concentration ( $C_{spike}$ ) of  $Br^-$  spike solution injected at the start of incubations, and the initial overlying water concentration of  $Br^-$  in excess of natural seawater  $Br^-$  ( $C_{ow}^0$ ):

$$V_{ow} = \frac{V_{spike} C_{spike}}{C_{ow}^0} \quad (1)$$

The value of  $C_{ow}^0$  was obtained by extrapolating the measured excess  $Br^-$  concentration in the overlying water to the start of the incubation using linear regression (Berelson et al., 1998; Jahnke and Jahnke, 2000). The flux of bromide into the sediment was calculated from the same regression as:

$$J = \left( \frac{\Delta C_{ow}}{\Delta t} \right) \frac{V_{ow}}{A} \quad (2)$$

where  $\Delta C_{ow}/\Delta t$  is the slope of the excess  $Br^-$  concentration in the overlying water versus incubation time and  $A$  is the sediment surface area.

The rate of porewater exchange ( $Q$ ) represents the volume of water that is exchanged per unit area per unit time, and is calculated as:

$$Q = \frac{J}{C_{ow}^0} \quad (3)$$

Therefore, the rate of porewater exchange by bioirrigation ( $I$ ) is calculated as the difference in porewater exchange rates in incubations with and without macrofauna:

$$I_{treatment} = Q_{treatment} - Q_{defaunated} \quad (4)$$

where “treatment” refers to intact cores or defaunated cores after lugworm addition.



In July, bioirrigation rates were determined as the difference between measured porewater exchange rates in the same core before and after lugworm addition. In November, it was not possible to compare  $Q$  in the same core under different treatments because of destructive sampling. Therefore, bioirrigation rates ( $I$ ) were calculated using the average exchange rate measured in defaunated cores before ( $Q^{\text{defaunated}}$ ) and after ( $Q^{\text{treatment}}$ ) lugworm addition. In November 2011,  $\text{Br}^-$  fluxes were not measured in cores P1 and P2 under intact conditions. Therefore, for these two incubations, porewater exchange rates are not available and overlying water volume was estimated as the average of that calculated in the other 3 cores, which varied only by 4% (CV).

Benthic fluxes of all other solutes were determined in a similar fashion (Eq. (2)), based on the overlying water volume, the known core cross-sectional area, and the slope of a linear regression of overlying water concentration vs. incubation time. Solute fluxes were corrected for dilution of the overlying water in each core with fresh seawater at each sampling time point. As a result of undiluted tracer solution remaining in the injection port, initial  $\text{Ca}^{2+}$  and  $\text{Br}^-$  concentrations were often anomalous and were not included in the final analysis.

#### 2.4. Porewater solute and solid phase distributions

In November 2011, replicate subcores (4 cm i.d.) were collected after flux measurements in two intact cores, three defaunated cores before lugworm addition, and three defaunated cores after lugworm addition. Subcores were extruded and sliced in an anaerobic glove box at 2.5 mm intervals from 0 to 2 cm, 5 mm intervals from 2 to 5 cm, and 1 cm intervals from 5 to 10 cm depth. Porosity was determined on one subcore. Corresponding depth sections from three additional replicate subcores were pooled in centrifuge tubes with built-in Whatman glass fiber filters, and centrifuged at 5000 rpm for 5 min. After centrifugation, centrifuge tubes were opened one at a time and porewater was dispensed through syringe filters (0.22  $\mu\text{m}$  PVDF) into sample containers. The remaining sediment was stored frozen for analysis of total and organic carbon content.

Sediment microsensor profiling was performed using commercial pH (100- $\mu\text{m}$  tip diameter) and  $\text{O}_2$  and  $\text{H}_2\text{S}$  microelectrodes (50- $\mu\text{m}$  tip diameter), operated with a motorized micromanipulator (Unisense A.S., Denmark). Oxygen microprofiles were made at 100  $\mu\text{m}$  resolution, with a 2-point calibration made in air-saturated seawater (100% saturation) and at depth in anoxic sediment (0% saturation). For  $\text{H}_2\text{S}$  and pH, depth profiles were made at 200  $\mu\text{m}$  resolution in the oxic zone, and 200 or 400  $\mu\text{m}$  resolution below. Calibrations for pH were made with three NBS standards and a TRIS buffer to correct for salinity effects (Dickson et al., 2007). pH is reported on the total scale. For  $\text{H}_2\text{S}$ , a 5-point calibration was made using  $\text{Na}_2\text{S}$  standards, which were prepared for each experiment, stored in an anaerobic glove box, and verified spectrophotometrically (Cline, 1969).  $\Sigma\text{H}_2\text{S}$  was calculated from  $\text{H}_2\text{S}$  based on pH measured at the same depth using the R package AquaEnv (Hofmann et al., 2010), with the relations of Millero (1995) for the thermodynamic equilibrium constant of  $\text{H}_2\text{S}$ .

Diffusive oxygen uptake (DOU) rates were calculated from porewater  $\text{O}_2$  microprofiles using Fick's first law:

$$J = -D_{\text{O}_2} \phi \frac{\partial[\text{O}_2]}{\partial z} \quad (5)$$

where  $z$  is depth and  $[\text{O}_2]$  denotes  $\text{O}_2$  concentration. The concentration gradient  $\partial[\text{O}_2]/\partial z$  was calculated as the linear slope in  $\text{O}_2$  concentration measured at the sediment-water interface, and adjusted for porosity ( $\phi$ ). The molecular diffusion coefficient ( $D^0$ )

was calculated at measured salinity and temperature using the R package *marelac* (Soetaert et al., 2012), and corrected for sediment tortuosity ( $D_{\text{O}_2} = D^0/\theta^2$ ) according to Archie's Law ( $\theta^2 = \phi^{1-m}$ , with  $m = 2$  for sands; Boudreau, 1997). DOU is compared with total oxygen uptake (TOU) rates derived from oxygen fluxes measured directly in core incubations (Section 2.3).

#### 2.5. Analytical methods

Sediment porosity was determined from water content and solid phase density measurements. Water content was determined by drying sediment samples to constant weight at 60 °C, and solid phase density measurements were based on volume displacement after adding a known mass of dry sediment to a graduated cylinder. Sediment grain size and sorting at the sampling site was measured in August 2011 by laser diffraction on a Malvern Mastersizer 2000.

Sediment samples were freeze-dried and ground to a fine powder for analysis of total carbon on a Thermo Scientific Delta V Elemental Analyzer ( $\pm 0.18\%$ ). Samples for total organic C were acidified with 0.1 N HCl for inorganic C removal prior to analysis, and total inorganic C was calculated by difference.

Overlying water samples were analyzed immediately upon collection for pH using an Orion ROSS glass electrode calibrated with NBS buffers and a seawater TRIS buffer prepared according to Dickson et al. (2007). Samples for  $\text{Br}^-$ ,  $\text{Ca}^{2+}$ , TA, and nutrients were 0.2  $\mu\text{m}$ -filtered and refrigerated until analysis. Phosphate ( $\text{PO}_4^{3-} \pm 3.5\%$ ), silicate ( $\text{Si}(\text{OH})_4 \pm 0.6\%$ ), nitrate ( $\text{NO}_3^- \pm 4.0\%$ ), nitrite ( $\text{NO}_2^- \pm 1.7\%$ ) and ammonium ( $\text{NH}_4^+ \pm 2.3\%$ ) concentrations in overlying water samples were measured using standard colorimetric methods on a Seal QuAatro autoanalyzer.  $\text{Br}^-$  ( $\pm 1.2\%$ ) was analyzed colorimetrically following the method of Presley (1971). TA ( $\pm 0.2\%$ ) was measured by Gran titration and  $\text{Ca}^{2+}$  ( $\pm 0.05\%$ ) in selected flux chamber incubations ( $n = 9$  in July,  $n = 11$  in November) by ethylene glycol tetraacetic acid (EGTA) titration (Tsunogai et al., 1968) using manual, scaled-down methods with an ultraprecision micrometer burette (Roger Gilmont Instruments). Replicate measurements of certified reference materials provided by A. G. Dickson (Dickson et al., 2003) and IAPSO seawater standard were used to validate the accuracy of TA and calcium measurements.

Dissolved inorganic carbon (DIC) was calculated from pH, TA, and nutrient concentrations at measured values of salinity and temperature with the R package AquaEnv (Hofmann et al., 2010), using the relations of Millero (2010) for the first and second dissociation constants of carbonic acid, Dickson and Riley (1979) for the dissociation constant of hydrogen fluoride, and Dickson (1990) for the dissociation constant of hydrogen sulfate. Calculated DIC concentrations in the overlying water of core incubations were used to determine the total DIC flux,  $J_{\text{DIC}}$ , using Equation (2). The net  $\text{CaCO}_3$  dissolution rate ( $R_{\text{CD}}$ ) was calculated as:

$$R_{\text{CD}} = J_{\text{TA}}(r_{\text{Ca:TA}}) \quad (6)$$

where  $r_{\text{Ca:TA}}$  is the average ratio of  $\text{Ca}^{2+}$ :TA flux measured in each treatment. Average values of  $r_{\text{Ca:TA}}$  were used because  $\text{Ca}^{2+}$  flux measurements were not available for all incubations. The DIC production due to organic matter remineralization ( $R_{\text{MIN}}$ ) was determined by subtracting the net  $\text{CaCO}_3$  dissolution rate ( $R_{\text{CD}}$ ) from the calculated total DIC flux.

$$R_{\text{MIN}} = J_{\text{DIC}} - R_{\text{CD}} \quad (7)$$

The ratio of C:N associated with organic matter remineralization was derived from  $R_{\text{MIN}}$  and the sum of dissolved inorganic nitrogen (DIN) fluxes in individual incubations. Finally, the efficiency of

metabolic dissolution ( $\epsilon_D$ ) is defined as the ratio of  $R_{CD}$  relative to  $R_{MIN}$  (Jahnke and Jahnke, 2004). As the portion of respiratory  $CO_2$  and metabolic acidity contributing to  $CaCO_3$  dissolution varies from 0 to 1,  $\epsilon_D$  is expected to vary between 0% and 100%.

Porewater samples collected in November 2011 were analyzed for TA at 0.3% precision. Acidified porewater samples (10  $\mu$ L of 6 N HCl per 1 mL sample) were analyzed for total dissolved Fe ( $\pm 1.1\%$ ) using a scaled-down Ferrozine method (Viollier et al., 2000) and for  $Ca^{2+}$  ( $\pm 0.1\%$ ) on a Perkin–Elmer ICP-OES.

Results are reported as the mean  $\pm 1$  standard deviation (s.d.) of  $n$  replicate measurements. Differences in solute fluxes and characteristic depths across seasons and treatments were identified using the Mann–Whitney  $U$  test.

### 3. Results

#### 3.1. Sediment properties

Sediments consisted of moderately sorted fine sand (median grain size 3.0  $\phi$ , sorting 0.7  $\phi$ ), composed of approximately 96% sand, with most of the remainder consisting of silt. Dry density was  $2.63 \pm 0.14$  g  $cm^{-3}$  ( $n = 5$ ), not significantly different from the theoretical density of pure quartz sand (i.e., 2.65 g  $cm^{-3}$ ). Sediment porosity was 0.47 in the top 0.5 cm, declined to 0.41 by 2 cm, and was nearly constant at this level to 10 cm. Sediment organic ( $0.23 \pm 0.08\%$  dry wt.) and inorganic carbon content ( $0.24 \pm 0.04\%$  dry wt.) were relatively constant with depth.

#### 3.2. Solute fluxes

Examples of time series results from defaunated core incubations before and after lugworm addition in July 2011 are shown in Fig. 2. Porewater exchange rates and solute fluxes measured in core incubations are reported in Table 1. Porewater exchange rates were lowest in defaunated cores and highest after lugworm addition. The effect of lugworms on porewater exchange was stronger in summer than in fall ( $U = 33$ ,  $n_1 = 8$ ,  $n_2 = 5$ ,  $p = 0.03$ ). Rates of total oxygen uptake (TOU) were also greater in summer than in fall ( $U = 39$  and  $U = 38$  in defaunated cores before and after lugworm addition respectively, with  $n_1 = 8$ ,  $n_2 = 5$ ,  $p < 0.01$ ), and lowest in defaunated cores (July:  $U = 63$ ,  $n_1 = n_2 = 8$ ,  $p < 0.001$ ; November:  $U = 24$ ,  $n_1 = n_2 = 5$ ,  $p < 0.01$ ).

Fluxes of  $NH_4^+$  and  $Si(OH)_4$  were directed into the overlying water, while  $NO_3^-$  fluxes were generally directed into the sediment

(Table 1).  $PO_4^{3-}$  fluxes were not different from zero in the absence of lugworms. Nutrient fluxes were greater in summer than in fall ( $U_{NH_4} = 32$  and  $38$ ,  $U_{PO_4} = 34$  and  $38$ ,  $U_{Si(OH)_4} = 39.5$  and  $40$  in defaunated cores before and after lugworm addition respectively, with  $n_1 = 8$ ,  $n_2 = 5$ ,  $p < 0.05$ ), with the exception of  $NO_3^-$  fluxes ( $U_{NO_3} = 14$  and  $p = 0.22$  in defaunated cores;  $U_{NO_3} = 5$  and  $p = 0.01$  after lugworm addition, with  $n_1 = 8$  and  $n_2 = 5$ ). Lugworm activity significantly enhanced the efflux of  $NH_4^+$  (July:  $U = 1$ ,  $n_1 = n_2 = 8$ ,  $p < 0.001$ ; November:  $U = 0$ ,  $n_1 = n_2 = 5$ ,  $p < 0.01$ ),  $PO_4^{3-}$  (July:  $U = 0$ ,  $n_1 = n_2 = 8$ ,  $p < 0.0001$ ; November:  $U = 3$ ,  $n_1 = n_2 = 5$ ,  $p = 0.03$ ) and  $Si(OH)_4$  (July:  $U = 0$ ,  $n_1 = n_2 = 8$ ,  $p < 0.0001$ ; November:  $U = 0$ ,  $n_1 = n_2 = 5$ ,  $p < 0.01$ ) and the influx of  $NO_3^-$  (July:  $U = 54$ ,  $n_1 = n_2 = 8$ ,  $p = 0.01$ ; November:  $U = 25$ ,  $n_1 = n_2 = 5$ ,  $p < 0.01$ ), with a greater effect in July than in November ( $U_{NH_4} = U_{PO_4} = 37$  at  $p < 0.01$ ;  $U_{Si} = 40$  at  $p < 0.001$ ;  $U_{NO_3} = 6$  at  $p = 0.02$  with  $n_1 = 8$  and  $n_2 = 5$ ).  $NH_4^+$  and  $Si(OH)_4$  efflux and  $NO_3^-$  influx were also greater in intact cores than in defaunated cores in November ( $U_{NH_4} = 24$ ,  $U_{Si(OH)_4} = 25$ ,  $U_{NO_3} = 0$  with  $n_1 = n_2 = 5$ ,  $p < 0.01$ ).

Lugworm activity enhanced the efflux of alkalinity ( $U = 64$ ,  $n_1 = n_2 = 8$ ,  $p < 0.0001$  in July, and  $U = 25$ ,  $n_1 = n_2 = 5$ ,  $p < 0.01$  in November) and calcium ( $U = 16$ ,  $n_1 = n_2 = 8$ ,  $p = 0.01$  in July, and  $U = 15$ ,  $n_1 = n_2 = 5$ ,  $p < 0.02$  in November), with a greater effect in July than in November ( $U = 34$  and  $p = 0.02$  for TA and  $U = 12$  and  $p = 0.03$  for  $Ca^{2+}$  with  $n_1 = 8$ ,  $n_2 = 5$ ) as shown in Table 1. In November,  $Ca^{2+}$  ( $U = 15$ ,  $n_1 = n_2 = 5$ ,  $p = 0.02$ ) and TA effluxes ( $U = 25$ ,  $n_1 = n_2 = 5$ ,  $p < 0.01$ ) in intact cores were greater than in defaunated cores, and similar to fluxes measured in defaunated cores after lugworm addition.

#### 3.3. Porewater solute distributions

Examples of  $O_2$ ,  $H_2S$ , and pH microprofiles in core incubations in July and November 2011 are shown in Fig. 3, and a summary of parameters derived from these measurements are reported in Table 1. Oxygen penetrated deeper in sediments in fall than in summer ( $U = 0$ ,  $n_1 = 9$ ,  $n_2 = 6$ ,  $p < 0.001$  in defaunated cores before lugworm addition and  $U = 23$ ,  $n_1 = 11$ ,  $n_2 = 10$ ,  $p = 0.01$  in defaunated cores after lugworm addition) and diffusive  $O_2$  uptake (DOU) was lower in fall ( $U = 54$ ,  $n_1 = 9$ ,  $n_2 = 6$ ,  $p < 0.001$  in defaunated cores before lugworm addition and  $U = 38.5$ ,  $n_1 = 6$ ,  $n_2 = 7$ ,  $p < 0.01$  in undisturbed sediments in defaunated cores after lugworm addition), except immediately over *Arenicola marina* faecal casts in defaunated cores after lugworm addition ( $U = 12$ ,  $n_1 = n_2 = 4$ ,

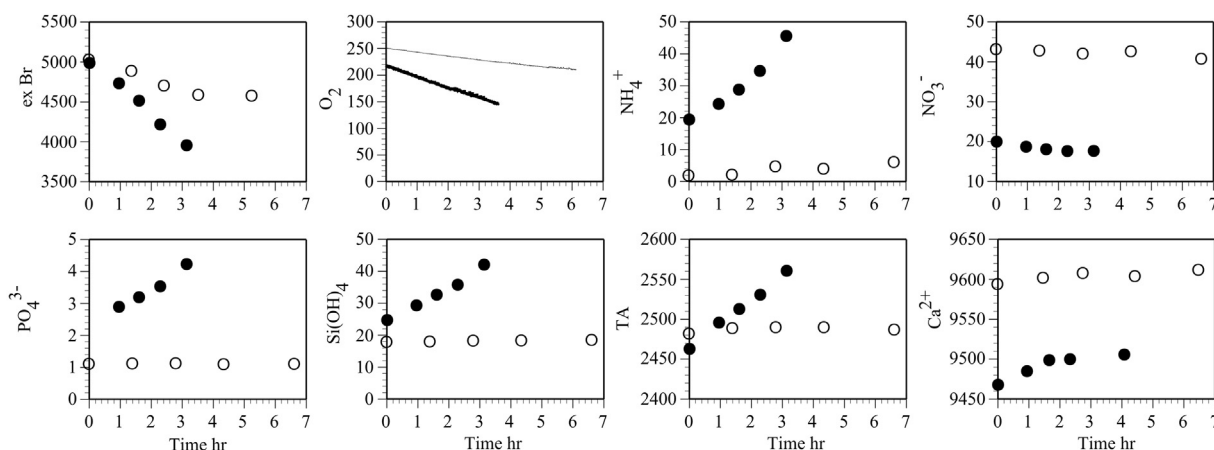


Fig. 2. Example time series results from defaunated core incubations before (open symbols,  $O_2$ : thin line) and after (filled symbols,  $O_2$ : thick line) the addition of *A. marina* in July 2011. Solute concentrations are expressed in  $\mu$ mol  $L^{-1}$ .

**Table 1**

Summary of porewater profiling and flux measurements in intact and defaunated core incubations before and after lugworm addition. Porewater profiling results from defaunated cores after lugworm addition are presented for undisturbed sediment patches (U) and microprofiles measured directly over *A. marina* fecal casts (F).

	July 2011		November 2011		
	Defaunated	+ Lugworms	Intact	Defaunated	+ Lugworms
Porewater exchange rate $L\ m^{-2}\ d^{-1}$	14.26 ± 13.95	73.07 ± 37.12	30.44 ± 5.06*	24.50 ± 13.57	45.67 ± 11.10
Measured fluxes $mmol\ m^{-2}\ h^{-1}$					
O <sub>2</sub>	−0.87 ± 0.18	−2.09 ± 1.06	−0.89 ± 0.21	−0.45 ± 0.11	−0.96 ± 0.39
NO <sub>3</sub> <sup>−</sup>	−0.01 ± 0.07	−0.09 ± 0.06	−0.04 ± 0.02	0.01 ± 0.00	−0.03 ± 0.02
NH <sub>4</sub> <sup>+</sup>	0.12 ± 0.08	0.94 ± 0.58	0.23 ± 0.10	0.08 ± 0.04	0.30 ± 0.15
PO <sub>4</sub> <sup>3−</sup>	0.00 ± 0.00	0.05 ± 0.02	0.00 ± 0.00	0.00 ± 0.00	0.01 ± 0.01
Si(OH) <sub>4</sub>	0.02 ± 0.00	0.32 ± 0.12	0.08 ± 0.02	0.01 ± 0.00	0.09 ± 0.03
TA	0.78 ± 0.55	3.63 ± 1.81	1.38 ± 0.41	0.31 ± 0.03	1.24 ± 0.52
Ca <sup>2+</sup>	0.22 ± 0.07	1.10 ± 0.12	0.57 ± 0.41	0.14 ± 0.05	0.79 ± 0.06
Calculated fluxes $mmol\ m^{-2}\ h^{-1}$					
DIC	0.72 ± 0.25	4.56 ± 2.14		0.53 ± 0.17	1.35 ± 0.63
R <sub>MIN</sub>	0.58 ± 0.19	3.57 ± 1.67		0.38 ± 0.18	0.73 ± 0.38
Calculated quotients					
RQ	−0.61 ± 0.11	−1.79 ± 0.73		−0.86 ± 0.45	−0.73 ± 0.19
C:N	6.12 ± 3.79	4.58 ± 1.17		4.36 ± 1.52	2.78 ± 0.88
ε <sub>D</sub>	22.27 ± 15.44	27.65 ± 5.94		54.54 ± 41.19	91.31 ± 18.08
Diffusive O <sub>2</sub> uptake $mmol\ m^{-2}\ h^{-1}$	−0.33 ± 0.07	U: −0.35 ± 0.08 F: −0.37 ± 0.05	−0.24 ± 0.25	−0.14 ± 0.03	U: −0.24 ± 0.05 F: −0.30 ± 0.15
O <sub>2</sub> penetration depth mm	1.17 ± 0.30	U: 1.06 ± 0.18 F: 1.38 ± 0.22	1.80 ± 0.35	2.73 ± 0.40	U: 1.85 ± 0.74 F: 1.68 ± 0.57
H <sub>2</sub> S horizon depth mm	15.78 ± 9.19	U: 13.74 ± 6.66 F: 21.05 ± 1.28	16.56 ± 4.47	5.1 ± 2.3	U: 3.27 ± 2.27 F: 7.15 ± 3.71
Incidence of surface pH peaks	9	U: 4 F: 0	1	1	U: 0 F: 1

$p = 0.17$ ). In the fall, DOU and O<sub>2</sub> penetration depth in defaunated cores after lugworm addition approached those measured in intact cores. Oxygen penetration depth was greater and DOU smaller in defaunated cores relative to both intact cores ( $U_{OPD} = 2$ ,  $n_1 = 10$ ,  $n_2 = 6$ ,  $p < 0.01$  and  $U_{DOU} = 2$ ,  $n_1 = 10$ ,  $n_2 = 6$ ,  $p = 0.001$ ) as well as cores with lugworms ( $U_{OPD} = 5.5$ ,  $n_1 = 10$ ,  $n_2 = 6$ ,  $p < 0.01$  and  $U_{DOU} = 3.5$ ,  $n_1 = 10$ ,  $n_2 = 6$ ,  $p = 0.002$ ). These differences were not significant in July.

The sulfide horizon in sediments was shallower in fall than in summer ( $U = 42$ ,  $n_1 = 9$ ,  $n_2 = 6$ ,  $p = 0.04$  and  $U = 103.5$ ,  $n_1 = 11$ ,  $n_2 = 10$ ,  $p < 0.001$  in defaunated cores before and after lugworm addition, respectively). Porewater pH generally declined with depth in the sediment, but replicate profiles in July revealed a distinct vertical pH distribution, with a surface peak at the bottom of the oxic zone and a strong sub-surface pH minimum deeper in the sediment. These characteristic pH profiles were observed in defaunated cores before lugworm addition and in undisturbed patches of sediment after lugworm addition (Table 1). This characteristic pH signature was not observed in November, except in one out of several replicate profiles measured in each treatment.

Total dissolved Fe distributions in porewater showed a subsurface maximum around 1 cm depth in the sediment in November (Fig. 4). Peak concentrations in defaunated cores were lower than in intact cores and in defaunated cores after lugworm addition. Porewater Ca<sup>2+</sup> profiles show a surface peak in all treatments (Fig. 4). Alkalinity profiles in intact cores show a concomitant surface maximum, followed by a broader maximum centered at about 5 cm depth (Fig. 4). Porewater TA distributions in defaunated cores increase with depth to high values between 8 and 10 mEq L<sup>−1</sup> at about 5 cm depth, and decrease only slightly below. After lugworm addition, porewater TA distributions at depth approach the values

observed in intact cores, with a subsurface peak between 1 and 2 cm depth.

## 4. Discussion

### 4.1. The impact of lugworm activity on porewater exchange

In this study, the activity of the lugworm *Arenicola marina* was determined by comparing porewater exchange rates measured by NaBr tracer fluxes in defaunated cores before and after lugworm addition as well as intact cores. The importance of porewater exchange due to lugworm activity, or bioirrigation, was demonstrated in summer and fall experiments, as exchange rates in defaunated cores increased after lugworm addition (Table 1). The lugworm bioirrigation rate ( $I$ ) was 59 L m<sup>−2</sup> d<sup>−1</sup> in July and 21 L m<sup>−2</sup> d<sup>−1</sup> in November. Bioirrigation was therefore stronger in summer, which may be due to a metabolic response of *A. marina* to the higher temperature associated with a higher O<sub>2</sub> supply needed due to stronger lugworm respiration, or due to more reducing conditions in sediments associated with higher microbial community respiration rates in sediments in summer, although this cannot be confirmed with our data. Porewater exchange in intact cores was also stronger than in defaunated cores in November (Table 1), resulting in a bioirrigation rate of 6 L m<sup>−2</sup> d<sup>−1</sup> associated with the natural macrofaunal community. The measured rates of bioirrigation are lower than previous estimates of lugworm bioirrigation rates (120–160 L m<sup>−2</sup> d<sup>−1</sup> at a population density of 50 individuals m<sup>−2</sup>, Kristensen, 2001). Low bioirrigation rates in defaunated cores after lugworm addition may be due to an inhibitory effect of accumulated reduced metabolites such as sulfide in sediment porewater on polychaete feeding and burrowing activities (Fuller, 1994). Alternately, this may be generally indicative of a

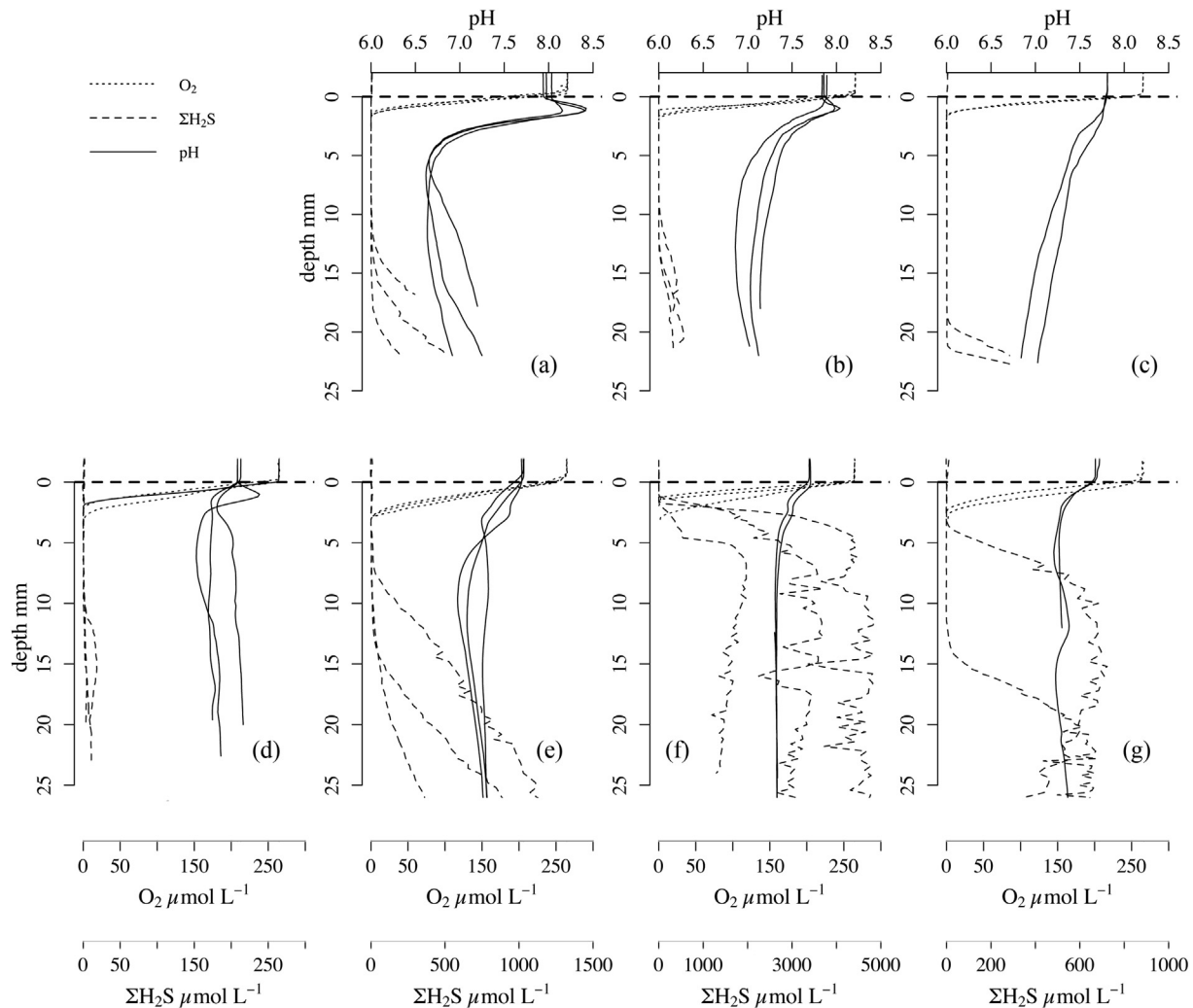


**Fig. 3.** Example porewater microprofiles from core incubations in July (top row) and November 2011 (bottom row), including measurements in intact (d) and defaunated cores before (a, e) and after lugworm addition (b, c, f, g). In defaunated cores after lugworm addition, examples of microprofiles measured in relatively undisturbed patches of sediment (b, f) and over *A. marina* fecal casts (c, g) are shown.

wall effect, or a change in the activity of macrofauna in an enclosure (e.g., Du Clos et al., 2013), which may also explain the low bioirrigation rates observed in intact cores. Measured porewater exchange rates are comparable to rates of porewater advection induced in permeable sands by wave and tidal pumping or bottom currents over sediment topography ( $0\text{--}100\text{ L m}^{-2}\text{ d}^{-1}$ , Precht and Huettel, 2003; Janssen et al., 2005).

The bioirrigation rates measured in core incubations yield individual pumping rates of  $0.52$  and  $0.19\text{ L ind}^{-1}\text{ d}^{-1}$  in July and November, respectively, given a sediment surface area of  $177\text{ cm}^2$  per core and a polychaete density of 2 individuals per core ( $\sim 120\text{ ind m}^{-2}$ ). Individual pumping rates vary depending on the size and activity of individuals, but measured rates are at the lower end of previously reported values, which range from  $0.4$  to  $3.2\text{ L ind}^{-1}\text{ d}^{-1}$  (Riisgård et al., 1996; Kristensen, 2001; Kristensen and Kostka 2005; Meysman et al., 2006; Na et al., 2008; Volkenborn et al., 2010). If the lugworm feeding pockets are at  $15\text{ cm}$  depth, then the flushing time for porewater above this horizon in the cores ( $1.09\text{ L}$ ) was about 1.0 day in July and 2.9 days in November. These estimates of porewater residence time provide an indication of the rapid timescale for the flushing of accumulated porewater metabolites in the defaunated cores after lugworm addition.

#### 4.2. The impact of lugworm activity on sediment community metabolism and nutrient fluxes

In both experiments and in all treatments, TOU in core incubations was greater than DOU as measured by microelectrode profiling (Table 1). High  $\text{O}_2$  consumption in intact cores and defaunated cores after the addition of *Arenicola marina* is likely a combined effect of respiration by lugworms and a stimulation of sediment community oxygen consumption by bioirrigation (enhanced solute transport) and bioturbation (enhanced particle mixing). By supplying dissolved  $\text{O}_2$  to deeper sediments (bioirrigation) and translocating reduced compounds from depth to the surface (bioturbation), lugworm activities enhance the  $\text{O}_2$  exposure of previously anoxic sediment and porewater and therefore increase the reoxidation of reduced metabolites in sediments (Banta et al., 1999; Forster et al., 1999; Kristensen, 2001). Polychaete burrows also enhance sediment community oxygen consumption by increasing sediment permeability, trapping labile organic material, and intensifying microbial respiration associated with organic-rich burrow linings (Wenzhöfer and Glud, 2004; Glud, 2008).

In defaunated cores, TOU and DOU were expected to be nearly equivalent, due to the absence of bioirrigation and bioturbation by macrofauna. Nevertheless, TOU was significantly greater than DOU

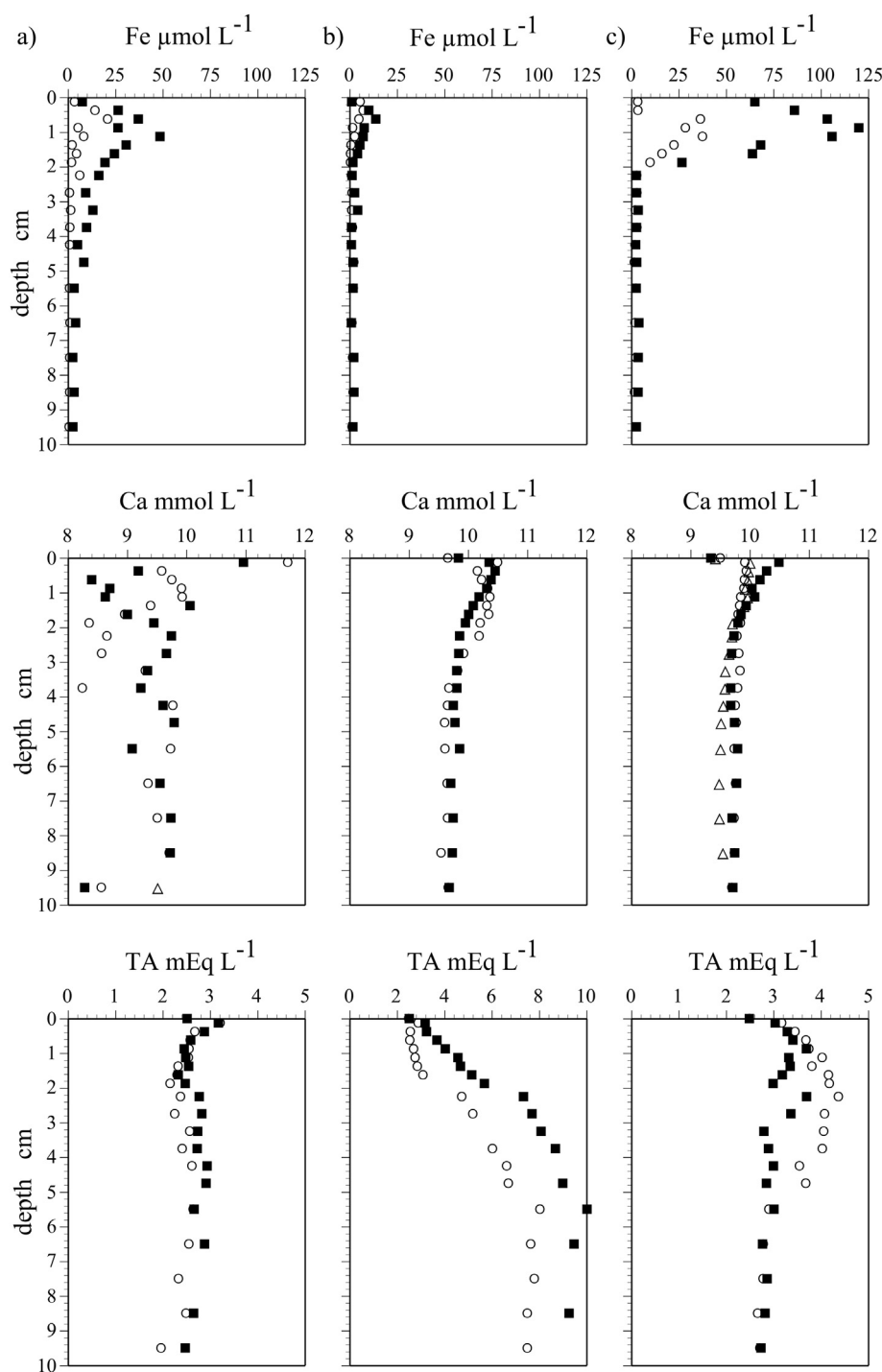


**Fig. 4.** Replicate porewater profiles of total dissolved Fe,  $\text{Ca}^{2+}$ , and TA measured in November 2011 in (a) intact cores and defaunated cores (b) before and (c) after lugworm addition.

in defaunated cores both in July ( $U = 72$ ,  $n_1 = 9$ ,  $n_2 = 8$ ,  $p < 0.001$ ) and November ( $U = 30$ ,  $n_1 = 6$ ,  $n_2 = 5$ ,  $p < 0.01$ ). The observed discrepancy between TOU and DOU in defaunated cores is likely due to a combination of factors, including sediment topography increasing interfacial surface area and residual bioturbation by meiofauna resistant to low  $\text{O}_2$  conditions. Indeed, living copepods were observed in November when opening cores after defaunation. By convention, fauna-mediated  $\text{O}_2$  uptake is calculated by subtracting DOU from TOU (Glud, 2008). Yet, the large discrepancy between TOU and DOU in the defaunated cores suggests that

processes other than lugworm activity influenced the DOU/TOU ratio. To estimate the lugworm-induced component of sediment  $\text{O}_2$  consumption, we therefore subtracted the TOU in defaunated cores from the TOU measured after lugworm addition. In this way, lugworms contributed an additional  $\text{O}_2$  uptake of 1.22 and 0.51  $\text{mmol m}^{-2} \text{h}^{-1}$  in July and November, representing 58% and 53% of TOU, respectively (Table 1). These estimates are on the low end of previously reported rates of fauna-mediated  $\text{O}_2$  uptake, which range widely from 0.3 to 7.7  $\text{mmol m}^{-2} \text{h}^{-1}$ , representing 10–80% of TOU (Forster and Graf, 1995; Kristensen, 2001; Webb



and Eyre, 2004; Na et al., 2008; D'Andrea and DeWitt, 2009; Volkenborn et al., 2010).

The shallower O<sub>2</sub> penetration, greater TOU, DOU and nutrient fluxes observed in July reflect a greater sediment community metabolic activity than in November (Table 1). This seasonal difference in benthic metabolism may be due to the higher ambient temperature or a greater labile organic matter content in sediments in summer. The effect of temperature alone can be approximated using an estimate of the temperature dependence of microbial respiration in sediments, represented by Q<sub>10</sub>, which designates the increase in respiration associated with a 10 °C increase in temperature. In coastal sediments, Q<sub>10</sub> is typically in the range of 2–3 (Therkildsen and Lomstein, 1993; Thamdrup and Fleischer, 1998; Hancke and Glud, 2004), so a temperature decrease of 4 °C from July to November would result in a decrease in sediment community metabolism by 31–55%. However, the observed decreases in O<sub>2</sub> uptake rates are 100% and greater, with the exception of DOU in defaunated cores after lugworm addition, suggesting that other factors may also contribute to the seasonal difference in sediment O<sub>2</sub> uptake.

One possible explanation for the large seasonal difference in sediment O<sub>2</sub> uptake may be an increased availability of labile organic matter in July relative to November, although this cannot be verified here. Another possible explanation is the transient oxidation of a reservoir of reduced compounds such as iron sulfides. In principle the respiratory quotient (RQ), which represents the ratio of C remineralized (R<sub>MIN</sub>) to O<sub>2</sub> consumed (TOU) by sediment community respiration, can be used to examine the degree of reoxidation of reduced compounds associated with anaerobic remineralization (Therkildsen and Lomstein, 1993). For example, the oxidation of Redfield organic matter to CO<sub>2</sub> and NO<sub>3</sub><sup>−</sup> will result in a RQ of 0.77 (Paulmier et al., 2009). In principle, RQ will increase with an increasing importance of suboxic and anaerobic respiratory pathways, such as denitrification, iron oxide reduction, and sulfate reduction, coupled to the burial of reduced metabolites in the form of iron sulfide minerals.

Measured RQ values in November did not change significantly after lugworm addition, and did not differ significantly from the decomposition of Redfield organic matter (Table 1), suggesting that reduced metabolites produced by anaerobic remineralization were efficiently reoxidized without significant burial of iron sulfide minerals. In defaunated cores in July, measured RQ was lower than that observed in November (Table 1). Although this difference was not significant ( $U = 22.5$ ,  $n_1 = 7$ ,  $n_2 = 10$ ,  $p = 0.12$ ), a higher O<sub>2</sub> uptake relative to DIC release in July may be attributed to the transient reoxidation of accumulated reduced compounds in sediments, associated with the activity of long distance electron transport (LDET, Risgaard-Petersen et al., 2012; see discussion in Section 4.5). After lugworm addition, higher and more variable values of RQ were observed in July, suggesting an enhanced non-steady-state flushing of DIC produced in deeper layers (Table 1), released by bioirrigation. This accumulated DIC was likely produced by anaerobic respiration, in general agreement with the large accumulation of alkalinity in deeper sediments in defaunated cores (Fig. 4). Therefore, the high RQ values observed in defaunated cores after lugworm addition in July may be an artifact of the short period (2 days) between lugworm addition and flux measurements, only twice the flushing time calculated for these cores by bioirrigation (see Section 4.1). In November, porewater solute distributions were likely at or near steady state at the time solute fluxes were measured in defaunated cores after lugworm addition due to lower respiration rates, despite an equivalent delay between lugworm addition and final flux measurements (6 days, equal to about twice the calculated flushing time of 2.9 days). This can explain the lower and less variable RQ values in defaunated cores after lugworm addition in November (Table 1).

Presumably, greater benthic metabolic activity in summer is expected to coincide with a shallower sulfide horizon due to higher rates of oxygen consumption and sulfate reduction in sediments. However in our experiments, the opposite was observed, with sulfide oxidation occurring deeper in sediments in July than in November (Table 1, Fig. 3). This may be due to the activity of LDET, a process capable of creating a wide suboxic zone, in July, as discussed in Section 4.4.

Lugworm activity enhanced the efflux of NH<sub>4</sub><sup>+</sup>, PO<sub>4</sub><sup>3−</sup>, and Si(OH)<sub>4</sub>, in agreement with a positive effect on total benthic metabolism (Huettel, 1990; Banta et al., 1999). In particular, measured DIN effluxes exceeded predictions based on rates of remineralization of Redfield ratio organic matter, resulting in C:N ratios generally below Redfield (6.6, Table 1). This trend is due to high NH<sub>4</sub><sup>+</sup> efflux relative to R<sub>MIN</sub>, which may have resulted from the delayed desorption of accumulated NH<sub>4</sub><sup>+</sup> in sediments produced by anaerobic respiration (Mackin and Aller, 1984).

Particle mixing by bioturbation also promotes the turnover of oxidants in sediments, by transporting reoxidized metabolites such as iron oxides to depth for reductive dissolution, and transporting reduced compounds such as iron sulfide minerals upward into the oxic surface layer for reoxidation. As such, sediment reworking activities enhance the reactive Fe content in coastal sediments and increase the relative importance of Fe(III) reduction in organic matter remineralization (Canfield et al., 1993; Kostka et al., 2002). The importance of bioturbation in maintaining an active Fe cycle in sediments was confirmed by the lower porewater Fe(II) concentrations observed in defaunated sediments in November, indicative of weaker Fe reduction rates, relative to intact sediments and defaunated sediments after lugworm addition (Fig. 4).

#### 4.3. Alkalinity production in sediments

Alkalinity generation in sediments, by denitrification and anaerobic respiration, is thought to account for an important fraction of CO<sub>2</sub> uptake in the North Sea (Thomas et al., 2009). With the high shellfish densities contributing biogenic CaCO<sub>3</sub> to sediments in the Oosterschelde (Coosen, 1986), one would expect that CaCO<sub>3</sub> dissolution may also represent an important source of TA in these sediments, which we evaluate here based on the ratio of Ca<sup>2+</sup> to TA efflux ( $r_{Ca:TA}$ ). This ratio is expected to approach ½ if CaCO<sub>3</sub> dissolution is the dominant source of TA in sediments, while lower ratios indicate important alternative TA sources such as denitrification or iron sulfide burial.

In November, the net TA release from sediments was almost entirely due to CaCO<sub>3</sub> dissolution ( $r_{Ca:TA} = 0.52 \pm 0.10$  for defaunated cores before and after lugworm addition and  $0.43 \pm 0.15$  for intact cores). However, porewater profiles measured in November suggested two separate TA sources in surface sediments and at depth (Fig. 4). In intact cores, overlapping Ca<sup>2+</sup> and TA maxima in surface sediments signaled a TA source associated with carbonate dissolution, while a second TA maximum between 3 and 6 cm depth was produced by organic matter remineralization coupled to iron and sulfate reduction. These anaerobic respiration pathways produce TA, Fe(II) and HS<sup>−</sup> at depth, which combine to form reduced sulfur minerals such as iron monosulfide (FeS) and pyrite (FeS<sub>2</sub>). The accumulation of these minerals results in the net production of TA at depth (Hu and Cai, 2011), which presumably obscured the surface TA maximum associated with carbonate dissolution in defaunated cores before and after lugworm addition (Fig. 4). Reoxidation of these reduced iron and sulfide compounds in the presence of O<sub>2</sub> limits their accumulation and releases acidity, thereby neutralizing TA produced by anaerobic respiration, lowering porewater saturation state ( $\Omega$ ) with respect to carbonate minerals, and promoting CaCO<sub>3</sub> dissolution. Deeper O<sub>2</sub> penetration

in November due to lower sediment metabolic rates (Table 1, Fig. 3) likely favored the reoxidation of reduced compounds, and therefore net TA production by carbonate dissolution.

In July,  $\text{CaCO}_3$  dissolution represented between 23 and 69% of the total TA flux from sediments ( $r_{\text{Ca:TA}} = 0.22 \pm 0.08$ ), with the exception of one core in which net calcification was observed. The remaining TA production in July may be due to net suboxic or anaerobic mineralization as discussed above, which should be most important in summer due to the greater benthic metabolic activity (Table 1). However, other TA sources may also have been important in July such as long distance electron transport, as will be discussed further below (Section 4.4).

Alkalinity and  $\text{Ca}^{2+}$  efflux were enhanced by macrofaunal activity (Table 1). To assess the potential role of this effect in natural sediments, it is important to examine whether the enhanced TA and  $\text{Ca}^{2+}$  fluxes measured in defaunated cores after lugworm addition may have been experimental artifacts associated with a transient release of solutes built up in sediment porewater during defaunation (Fig. 4), or the non-steady-state reoxidation of reduced metabolites that accumulated in sediments during defaunation, resulting in the acidification of sediment porewater and enhanced  $\text{CaCO}_3$  dissolution. An important obstacle in evaluating such transient effects in this study is that bioirrigation is inherently a non-steady state process.

Here, an equilibration period equivalent to about 2 times the residence time of porewater with respect to measured bioirrigation rates ( $\tau_{\text{res}}$ ) was included in the experimental design, before the measurement of solute fluxes and porewater solute distributions after lugworm addition to defaunated cores, to permit porewater solute distributions to re-equilibrate with bioirrigation. As observed in the November experiment, porewater distributions of  $\text{Ca}^{2+}$ , TA and  $\text{Fe}^{2+}$  measured after lugworm addition approach those measured in intact cores (Fig. 4). This suggests that the equilibration period was sufficient to re-establish equilibrium in the porewater carbonate system, and the observed effect of bioirrigation on solute fluxes was not a transient one. This is consistent with the observation that  $\text{Ca}^{2+}$  and TA fluxes measured in defaunated cores after lugworm addition in November approached those measured in intact cores prior to defaunation, which were both  $>3\times$  higher than fluxes in defaunated cores. In July, solute fluxes in intact cores and porewater  $\text{Ca}^{2+}$ , TA and  $\text{Fe}^{2+}$  distributions were not measured. However, the effect of lugworm addition in July was similar to that observed in November, resulting in a 4.7- and 4.0-fold increase in TA flux in July and November, and a 5.0-fold and 5.6-fold increase in  $\text{Ca}^{2+}$  flux in July and November. Based on (1) the similarity in the effect of lugworms on TA and  $\text{Ca}^{2+}$  fluxes in July and November, (2) the similarity in the relative equilibration period between lugworm addition in defaunated cores and the measurement of solute fluxes in July and November (about  $2\tau_{\text{res}}$ ), and (3) the similarity in porewater solute distributions in intact and defaunated cores after lugworm addition in November, we infer that the observed effect of lugworm activity on  $\text{Ca}^{2+}$  and alkalinity flux was not likely an experimental artifact. This conclusion is confirmed by the observation of transient TA fluxes for 2.8 days immediately following lugworm addition to defaunated cores collected in November 2011 (see Supplementary Material), only slightly less than the 2.9 day  $\tau_{\text{res}}$  calculated for the November experiment (Section 4.1).

The release of  $\text{Ca}^{2+}$  and TA from Oosterschelde intertidal sediments is indicative of  $\text{CaCO}_3$  dissolution resulting from the production of metabolic acidity in these sediments, since coastal surface waters are supersaturated with respect to  $\text{CaCO}_3$ . Lugworm activity enhanced metabolic dissolution efficiency (Table 1), although the effect was significant only in November ( $U = 21$ ,  $n_1 = n_2 = 5$ ,  $p = 0.05$ ). It is interesting to note that the response of

metabolic dissolution efficiency,  $\varepsilon_D$ , to lugworm activity runs counter to the effect of porewater advection in biogenic carbonate sands. Rao et al. (2012) reported a decrease in metabolic  $\text{CaCO}_3$  dissolution efficiency with increased porewater advection in reef sands due to the reduced residence time of metabolic acidity in porewater. In terrigenous sediments, however, carbonate cycling is intimately linked to coupled Fe and S cycling (Thomas et al., 2009; Faber et al., 2012). It is likely that both porewater flushing and particle reworking by lugworms increase  $\varepsilon_D$  in Oosterschelde sands, as observed in November, by favoring aerobic mineralization and the reoxidation of reduced compounds in sediments as discussed above (Banta et al., 1999), enhancing the production of acidity relative to total benthic metabolism, and increasing the sediment volume exposed to undersaturated conditions with respect to  $\text{CaCO}_3$ . The absence of a significant effect of lugworm activity on  $\varepsilon_D$  in July may be attributed to a potentially confounding effect resulting from the development of LDET in core incubations in July, which will be discussed in the next section.

#### 4.4. The development of long distance electron transport in core incubations

It has recently been proposed that the pH distribution in coastal sediments can be altered by long distance electron transport (LDET), mediated by electrogenic filamentous bacteria, which couples spatially separated redox half-reactions (Nielsen et al., 2010). These newly discovered sulfur-oxidizing bacteria, belonging to the Desulfobulbaceae family (Pfeffer et al., 2012), can remove sulfide down to 1–2 cm depth in the sediment and reduce  $\text{O}_2$  near the sediment-water interface, thus potentially creating a large suboxic zone. The local proton production and consumption associated with these oxidation and reduction half-reactions generate distinctive porewater pH signatures, as observed in Oosterschelde core incubations in July. Sharp pH peaks in darkened, oxic surface sediments overlying a thick suboxic zone are an important indication of proton consumption associated with oxygen uptake by LDET, since all other processes occurring in the oxic zone are known to generate protons, with the exception of photosynthesis (Nielsen et al., 2010). The pH minimum at depth associated with sulfide oxidation by LDET has been observed to stimulate the dissolution of carbonates and iron sulfides (Risgaard-Petersen et al., 2012). The remobilized  $\text{Ca}^{2+}$  and  $\text{Fe}^{2+}$  subsequently diffuse upward into the oxic zone, where they are deposited as high Mg calcite and iron oxide minerals. In this way, LDET promotes carbonate and iron cycling in coastal sediments, and therefore may also play an important role in alkalinity generation, modulating benthic fluxes of dissolved inorganic carbon and alkalinity.

We infer that LDET is active in July but negligible in November based on porewater microprofiles measured in core incubations (Table 1, Fig. 3). Porewater pH distributions with peaks at the base of the oxic zone and minima in deeper suboxic layers, characteristic of LDET, were predominantly observed in July, and only on rare occasions in November. Other possible explanations for surface pH maxima at the base of the oxic zone include 1) photosynthesis, which we have excluded in this experiment by conducting incubations in darkness, and 2) the aerobic oxidation of sulfide to elemental sulfur, which can be excluded here given the absence of sulfide in the upper 1–2 cm of  $\text{H}_2\text{S}$  profiles measured in parallel. Therefore, we consider that LDET is the most likely explanation for these porewater pH profiles. Indeed, Nielsen et al. (2010) first described this distinctive pH signature and concluded, based on similar measurements in core incubations, that these observations are an important indication of LDET in sediments.

The occurrence of LDET explains the higher TOU, DOU, and RQ, shallower OPD and deeper sulfide horizons observed in defaunated

cores in July relative to November. Note also that metabolic dissolution efficiency,  $\varepsilon_D$ , was generally lower in July relative to November. One explanation for this may stem from the occurrence of LDET in July. While low pH conditions induced by LDET in deeper sediments stimulate  $\text{CaCO}_3$  dissolution, the high porewater pH and  $\Omega$  produced by LDET in surface sediments promotes interfacial calcification (Risgaard-Petersen et al., 2012), and may thereby reduce net metabolic carbonate dissolution and  $\varepsilon_D$  in summer. It is not possible to determine the relative importance of LDET and remineralization in controlling  $\varepsilon_D$  at this time, but the potential importance of LDET in sediment TA generation warrants further study.

In July, the porewater LDET signature described above was strongest in defaunated cores prior to lugworm addition, with weaker and less frequent signals observed after lugworm addition only between fecal casts. This observation confirms that bioturbation by benthic fauna disrupts LDET, as discussed by Malkin et al. (2014) and suggested by Nielsen et al. (2010). The indication that LDET developed in summer but not in the fall also suggests the potential importance of seasonality on LDET development.

#### 4.5. Conclusions

Our results confirm previous reports of enhanced benthic metabolism and nutrient fluxes in the presence of burrowing infauna such as *Arenicola marina*, and demonstrate for the first time, the positive effect of biological mixing on alkalinity production in intertidal sediments. Two *ex situ* experiments in July and November 2011 revealed the importance of seasonality in the biogeochemistry of Oosterschelde sediments. Greater benthic metabolic activity in summer, likely due to higher temperatures, led to higher remineralization and  $\text{O}_2$  consumption rates, shallower  $\text{O}_2$  penetration, higher nutrient,  $\text{Ca}^{2+}$  and TA fluxes than in the fall. Stronger bioirrigation in summer also resulted in a more pronounced positive effect of *A. marina* on interfacial solute fluxes than in the fall. An unexpected result was the indication of microbial long distance electron transport in these sediments in summer.

Our measurements provide direct confirmation of a strong alkalinity source in coastal North Sea sediments, which was previously suggested by extensive water column surveys (Thomas et al., 2009). Assuming the observed TA production rates measured in this study are representative, and integrating this benthic TA production rate over the intertidal area of the southern North Sea (approximately 5000 km<sup>2</sup>) implies an annual alkalinity source of 53–160 Gmol. This corresponds reasonably well with the estimate of Thomas et al. (2009) of 73 Gmol TA produced annually in the Wadden Sea. On the ecosystem scale, benthic alkalinity generation buffers  $\text{CO}_2$  release by autochthonous  $\text{CaCO}_3$  production and organic matter decomposition in the water column and in sediments, therefore facilitating a net  $\text{CO}_2$  drawdown from the atmosphere (Thomas et al., 2009). It is therefore critical to understand the biogeochemical processes responsible for alkalinity production in coastal sediments.

Alkalinity production in intertidal Oosterschelde sediments was entirely due to carbonate dissolution in the fall, with other processes, including anaerobic respiration and LDET, playing an important role in summer. In agreement with previous studies, sediment reworking enhanced Fe turnover in sediments. The effect of lugworm mixing on Fe reoxidation and porewater  $\text{O}_2$  supply, and the ensuing production of metabolic acidity in surface sediments may also explain the observed increase in metabolic  $\text{CaCO}_3$  dissolution efficiency in the presence of biological mixing in the fall. A similar response of dissolution efficiency,  $\varepsilon_D$ , was not observed in summer, however, when  $\varepsilon_D$  was generally lower, either due to

greater net anaerobic respiration rates or to enhanced interfacial calcification associated with LDET.

The importance of carbonate dissolution in fueling alkalinity production in Oosterschelde sediments is noteworthy in view of previous reports that anaerobic respiration and denitrification represent the dominant alkalinity sources in sediments (Thomas et al., 2009; Hu and Cai, 2011). Our results underscore the importance of sediment geochemical composition and the mode of porewater and particle mixing, which are likely to account for much variability in the relative importance of different benthic alkalinity sources (Krumins et al., 2013).

#### Acknowledgments

This research was funded by an Odysseus grant (FWO, Belgium), VIDI grant 864.08.004 (NWO, The Netherlands) and ERC Starting Grant 2012-306933 to FJRM. The authors thank Pieter van Rijswijk and Silvia Hidalgo Martínez for help with field and laboratory sampling, Jan Sinke, Marco Houtekamer, Yvonne van der Maas, and Pieter van Breughel for analytical assistance, and Annette Wielemaker for map preparation.

#### Appendix A. Supplementary data

Supplementary data related to this article can be found at <http://dx.doi.org/10.1016/j.ecss.2014.06.006>.

#### References

- Banta, G.T., Holmer, M., Jensen, M.H., Kristensen, E., 1999. Effects of two polychaete worms, *Nereis diversicolor* and *Arenicola marina*, on aerobic and anaerobic decomposition in a sandy marine sediment. *Aquat. Microb. Ecol.* 19, 189–204.
- Bates, N.R., Mathis, J.T., 2009. The Arctic Ocean marine carbon cycle: evaluation of air-sea  $\text{CO}_2$  exchanges, ocean acidification impacts and potential feedbacks. *Biogeosciences* 6, 2433–2459.
- Berelson, W., Heggie, D., Longmore, A., Kilgore, T., Nicholson, G., Skyring, G., 1998. Benthic nutrient recycling in port Phillip Bay, Australia. *Estuar. Coast. Shelf Sci.* 46, 917–934.
- Boudreau, B.P., 1997. *Diagenetic Models and Their Implementation*. Springer.
- Canfield, D.E., Jørgensen, B.B., Fossing, H., Glud, R., Gundersen, J., Ramsing, N.B., Thamdrup, B., Hansen, J.W., Nielsen, L.P., Hall, P.O.J., 1993. Pathways of organic carbon oxidation in three continental margin sediments. *Mar. Geol.* 113, 27–40.
- Cline, J.D., 1969. Spectrophotometric determination of hydrogen sulfide in natural waters. *Limnol. Oceanogr.* 14, 454–458.
- Coosen, J., 1986. Biomass and density fluctuations of the macrozoobenthos of the intertidal flats in the Oosterschelde, The Netherlands. *Hydrobiologia* 142, 338.
- Coosen, J., Seys, J., Meire, P.M., Craeymeersch, J., 1994. Effect of sedimentological and hydrodynamical changes in the intertidal areas of the Oosterschelde estuary (SW Netherlands) on distribution, density and biomass of some common macrobenthic species. *Hydrobiologia* 282/283, 235–249.
- D'Andrea, A.F., DeWitt, T.H., 2009. Geochemical ecosystem engineering by the mud shrimp *Upogebia pugettensis* (Crustacea: Thalassinidae) in Yaquina Bay, Oregon: density-dependent effects on organic matter remineralization and nutrient cycling. *Limnol. Oceanogr.* 54, 1911–1932.
- de Beer, D., Wenzhöfer, F., Ferdelman, T.G., Boehme, S.E., Huettel, M., 2005. Transport and mineralization rates in North Sea sandy intertidal sediments, Sylt-Rømø Basin, Wadden Sea. *Limnol. Oceanogr.* 50, 113–127.
- de Jong, D., Nienhuis, P., Kater, B., 1994. Microphytobenthos in the Oosterschelde estuary (The Netherlands) 1981–1990; consequences of a changed tidal regime. *Hydrobiologia* 282/283, 183–195.
- Dickson, A.G., Riley, J.P., 1979. The estimation of acid dissociation constants in seawater media from potentiometric titrations with strong base. I. The ionic product of water. *Mar. Chem.* 7, 89–99.
- Dickson, A.G., 1990. Standard potential of the reaction:  $\text{AgCl(s)} + 1/2\text{H}_2\text{(g)} = \text{Ag(s)} + \text{HCl(aq)}$ , and the standard acidity constant of the ion  $\text{HSO}_4^-$  in synthetic sea water from 273.15 to 318.15 K. *J. Chem. Thermodyn.* 22, 113–127.
- Dickson, A.G., et al., 2003. Reference materials for oceanic  $\text{CO}_2$  analysis: a method for the certification of total alkalinity. *Mar. Chem.* 80, 185–197.
- Dickson, A.G., Sabine, C.L., Christian, J.R., 2007. Guide to best practices for ocean  $\text{CO}_2$  measurements. In: *PICES Special Publication*, vol. 3, 191 pp.
- Du Clos, K.T., Lindsay, S.M., Jumars, P.A., 2013. Spatial distribution of *Alitta virens* and *Clymenella torquata* with respect to rigid boundaries in mud and sand. *J. Mar. Res.* 71, 211–226.
- Faber, P., Kessler, A., Bull, J., McKelvie, I., Meysman, F., Cook, P., 2012. The role of alkalinity generation in controlling the fluxes of  $\text{CO}_2$  during exposure and inundation on tidal flats. *Biogeosciences* 9, 4087–4097.



- Feely, R.A., Sabine, C.L., Hernandez-Ayon, J.M., Janson, D., Hales, B., 2008. Evidence for upwelling of corrosive "acidified" water onto the continental shelf. *Science* 320 (5882), 1490–1492.
- Feely, R.A., Alin, S., Newton, J., Sabine, C., Warner, M., Krembs, C., Maloy, C., 2010. The combined effects of ocean acidification, mixing, and respiration on pH and carbonate saturation in an urbanized estuary. *Estuar. Coast. Shelf Sci.* 88, 442–449.
- Forster, S., Graf, G., 1995. Impact of irrigation on oxygen flux into the sediment: intermittent pumping by *Callianassa subterranea* and 'piston-pumping' by *Janice conchilega*. *Mar. Biol.* 123, 335–346.
- Forster, S., Glud, R., Gundersen, J., Huettel, M., 1999. In situ study of bromide tracer and oxygen flux in coastal sediments. *Estuar. Coast. Shelf Sci.* 49, 813–827.
- Forster, P., Ramaswamy, V., Artaxo, P., Bernsten, T., Betts, R., Fahey, D.W., Haywood, J., Lean, J., Lowe, D.C., Myhre, G., Nganga, J., Prinn, R., Raga, G., Schulz, M., Van Dorland, R., 2007. Changes in atmospheric constituents and in radiative forcing. In: Solomon, S., Qin, D., Manning, M., Chen, Z., Marquis, M., Averyt, K.B., Tignor, M., Miller, H.L. (Eds.), *Climate change 2007: the Physical Science Basis, Contribution of Working Group I to the Fourth Assessment Report of the Intergovernmental Panel on Climate Change*. Cambridge University Press, Cambridge, United Kingdom and New York, NY, USA.
- Fuller, C.M., 1994. Effects of porewater hydrogen sulfide on the feeding activity of the subsurface deposit-feeding polychaete, *Clymenella torquata*. *Leidy. J. Mar. Res.* 52, 1101–1127.
- Gazeau, F., Quiblier, C., Jansen, J., Gattuso, J.-P., Middelburg, J., Heip, C., 2007. Impact of elevated CO<sub>2</sub> on shellfish calcification. *Geophys. Res. Lett.* 34, L07603.
- Glud, R.N., 2008. Oxygen dynamics of marine sediments. *Mar. Biol. Res.* 4, 243–289.
- Guinotte, J.M., Fabry, V.J., 2008. Ocean acidification and its potential effects on marine ecosystems, pp. 320–342. In: ] (Ed.), *The Year in Ecology and Conservation Biology 2008*. Annals of the New York Academy of Sciences. Ostfeld, R.S. and Schlesinger, W.H. ].
- Hancke, K., Glud, R., 2004. Temperature effects on respiration and photosynthesis in three diatom-dominated benthic communities. *Aquat. Microb. Ecol.* 37, 265–281.
- Hofmann, A., Soetaert, K., Middelburg, J., Meysman, F., 2010. AquaEnv: an aquatic acid-base modelling environment in R. *Aquat. Geochem.* 16 (4), 507–546.
- Hu, X., Cai, W.-J., 2011. An assessment of ocean margin anaerobic processes on oceanic alkalinity budget. *Glob. Biogeochem. Cycles* 25, GB3003. <http://dx.doi.org/10.1029/2010GB003859>.
- Hutchins, D.A., Mulholland, M.R., Fu, F., 2009. Nutrient cycles and marine microbes in a CO<sub>2</sub>-enriched ocean. *Oceanography* 22, 128–145.
- Huettel, M., 1990. Influence of the lugworm *Arenicola marina* on porewater nutrient profiles of sand flat sediments. *Mar. Ecol. Prog. Ser.* 62, 241–248.
- Jahnke, R.A., Jahnke, D.B., 2004. Calcium carbonate dissolution in deep sea sediments: reconciling microelectrode, pore water and benthic flux chamber results. *Geochim. Cosmochim. Acta* 68, 47–59.
- Jahnke, R.A., Jahnke, D.B., 2000. Rates of C, N, P and Si recycling and denitrification at the US Mid-Atlantic continental slope depocenter. *Deep-Sea Res.* 47, 1405–1428.
- Janssen, F., Huettel, M., Witte, U., 2005. Pore-water advection and solute fluxes in permeable marine sediments (I): calibration and performance of the novel benthic chamber system *Sandy*. *Limnol. Oceanogr.* 50, 768–778.
- Kostka, J.E., Gribsholt, B., Petrie, E., Dalton, D., Skelton, H., Kristensen, E., 2002. The rates and pathways of carbon oxidation in bioturbated saltmarsh sediments. *Limnol. Oceanogr.* 47, 230–240.
- Kristensen, E., 1988. Benthic fauna and biogeochemical processes in marine sediments: microbial activities and fluxes. In: Blackburn, T.H., Sørensen, J. (Eds.), *Nitrogen Cycling in Coastal Marine Environments*. John Wiley & Sons Ltd, pp. 275–299.
- Kristensen, E., 2001. Impact of polychaetes (*Nereis* spp. and *Arenicola marina*) on carbon biogeochemistry in coastal marine sediment: a review. *Geochim. Trans.* 2, 92–104.
- Kristensen, E., Kostka, J., 2005. Macrofaunal burrows and irrigation in marine sediment: microbiological and biogeochemical interactions. In: Kristensen, E., Haese, R.R., Kostka, J. (Eds.), *Interactions between Macro- and Microorganisms in Marine Sediments*. American Geophysical Union, Washington, DC, pp. 125–157.
- Kristensen, E., Penha-Lopes, G., Delefosse, M., Valdemarsen, R., Quintana, C., Banta, G., 2012. What is bioturbation? the need for a precise definition for fauna in aquatic sciences. *Mar. Ecol. Prog. Ser.* 446, 285–302.
- Kroeker, K., Kordas, R., Crim, R., Hendriks, I., Ramajo, L., Singh, G., Duarte, C., Gattuso, J.-P., 2013. Impacts of ocean acidification on marine organisms: quantifying sensitivities and interaction with warming. *Glob. Change Biol.* 19, 1884–1896.
- Krummins, V., Gehlen, M., Arndt, S., Van Cappellen, P., Regnier, P., 2013. Dissolved inorganic carbon and alkalinity fluxes from coastal marine sediments: model estimates for different shelf environments and sensitivity to global change. *Biogeochemistry* 10, 371–398.
- Mackin, J.E., Aller, R.C., 1984. Ammonium adsorption in marine sediments. *Limnol. Oceanogr.* 29, 250–257.
- Malkin, S.Y., Rao, A.M.F., Seitaj, D., Vasquez-Cardenas, D., Zetsche, E.-M., Boschker, H.T.S., Meysman, F.J.R., 2014. Natural occurrence of microbial sulphur oxidation by long-range electron transport in the seafloor. *ISME J.* <http://dx.doi.org/10.1038/ismej.2014.41>.
- Meysman, F.J.R., Galaktionov, O.S., Gribsholt, B., Middelburg, J.J., 2006. Bioirrigation in permeable sediments: advective pore-water transport induced by burrow ventilation. *Limnol. Oceanogr.* 51, 142–156.
- Millero, F.J., 1995. Thermodynamics of the carbon dioxide system in the oceans. *Geochim. Cosmochim. Acta* 59, 661–677.
- Millero, F.J., 2010. Carbonate constant for estuarine waters. *Mar. Freshw. Res.* 61, 139–142.
- Na, T., Gribsholt, B., Galaktionov, O., Lee, R., Meysman, F., 2008. Influence of advective bioirrigation on carbon and nitrogen cycling in sandy sediments. *J. Mar. Res.* 66, 691–722.
- Nielsen, L., Risgaard-Petersen, N., Fossing, H., Christensen, P., Sayama, M., 2010. Electric currents couple spatially separated biogeochemical processes in marine sediment. *Nature* 463, 1071–1074.
- Nienhuis, P., Smaal, A., 1994. The Oosterschelde estuary, a case-study of a changing ecosystem: an introduction. *Hydrobiologia* 282/283, 1–14.
- Paulmier, A., Kries, I., Oeschle, A., 2009. Stoichiometries of remineralisation and denitrification in global biogeochemical ocean models. *Biogeochemistry* 6, 923–935.
- Pfeffer, C., Larsen, S., Song, J., Dong, M., Besenbacher, F., Meyer, R.L., Kjeldsen, K.U., Schreiber, L., Gorby, Y.A., El-Naggar, M.Y., Leung, K.M., Schramm, A., Risgaard-Petersen, N., Nielsen, L.P., 2012. Filamentous bacteria transport electrons over centimetre distances. *Nature* 491, 218–221.
- Precht, E., Huettel, M., 2003. Advective pore-water exchange driven by surface gravity waves and its ecological implications. *Limnol. Oceanogr.* 48, 1674–1684.
- Presley, B.J., 1971. Techniques for analyzing interstitial water samples. Part I. Determination of selected minor and major inorganic constituents. In: Winterer, E.L., Riedel, W.R., Brönnimann, P., Gealy, E., Heath, G., Kroenke, L., Martini, E., Moberly Jr., R., Resig, J., Worsley, T. (Eds.), *Initial Reports of the Deep Sea Drilling Project*, v. 7. U. S. Government Printing Office, pp. 1749–1755.
- Rao, A., Polerecky, L., Ionescu, D., Meysman, F.J.R., de Beer, D., 2012. The influence of physically-induced porewater advection, benthic photosynthesis and respiration on CaCO<sub>3</sub> dynamics in reef sands. *Limnol. Oceanogr.* 57 (3), 809–825.
- Reise, K., Herre, E., Sturm, M., 1994. Biomass and abundance of macrofauna in intertidal sediments of Königshafen in the northern Wadden Sea. *Helgoländer Meeresunters.* 48, 201–215.
- Riisgård, H.U., Berntsen, I., Tarp, B., 1996. The lugworm (*Arenicola marina*) pump: characteristics, modelling and energy cost. *Mar. Ecol. Prog. Ser.* 138, 149–156.
- Risgaard-Petersen, N., Revil, A., Meister, P., Nielsen, L., 2012. Sulfur, iron-, and calcium cycling associated with natural electric currents running through marine sediment. *Geochim. Cosmochim. Acta* 92, 1–13.
- Roy, H., Lee, J., Jansen, S., de Beer, D., 2008. Tide-driven deep pore-water flow in intertidal sand flats. *Limnol. Oceanogr.* 53 (4), 1521–1530.
- Sabine, C., Feely, R., Gruber, N., Key, R., Lee, K., Bullister, J., Wanninkhof, R., Wong, C., Wallace, D., Tilbrook, B., Millero, F., Peng, T., Kozyr, A., Ono, T., Rios, A., 2004. The oceanic sink for anthropogenic CO<sub>2</sub>. *Science* 305, 367–371.
- Seys, J., Meire, P., Coosen, J., Craeymeersch, J., 1994. Long-term changes (1979–1989) in the intertidal macrozoobenthos of the Oosterschelde estuary: are patterns in total density, biomass and diversity induced by the construction of the storm-surge barrier? *Hydrobiologia* 282/283, 251–264.
- Stumm, W., Morgan, J.J., 1996. *Aquatic Chemistry: Chemical Equilibria and Rates in Natural Waters*. third Ed. John Wiley & Sons, New York, p. 1040.
- Soetaert, K., Petzoldt, T., Meysman, F.J.R., 2012. Package 'marelac': Tools for aquatic sciences. v.2.1.2.
- ten Brinke, W., Dronkers, J., Mulder, J., 1994. Fine sediments in the Oosterschelde tidal basin before and after partial closure. *Hydrobiologia* 282/283, 41–56.
- Thamdrup, B., Fleischer, S., 1998. Temperature dependence of oxygen respiration, nitrogen mineralization, and nitrification in Arctic sediments. *Aquat. Microb. Ecol.* 15, 191–199.
- Therkildsen, M., Lomstein, B., 1993. Seasonal variation in net benthic C mineralization in a shallow estuary. *FEMS Microbiol. Ecol.* 12, 131–142.
- Thomas, H., Schiettecatte, L.-S., Suykens, K., Koné, Y., Shadwick, E., Prowse, A., Bozec, Y., de Baar, H., Borges, A., 2009. Enhanced ocean carbon storage from anaerobic alkalinity generation in coastal sediments. *Biogeochemistry* 6, 267–274.
- Tsunogai, S., Nishimura, M., Nakaya, S., 1968. Complexometric titration of calcium in the presence of larger amounts of magnesium. *Talanta* 15, 385–390.
- Viollier, E., Inglett, P., Hunter, K., Roychoudhury, A., Van Cappellen, P., 2000. The ferrozine method revisited: Fe(II)/Fe(III) determination in natural waters. *Appl. Geochem.* 15, 785–790.
- Volkenborn, N., Polerecky, L., Hedtkamp, S., Beusekom, J., de Beer, D., 2007. Bioturbation and bioirrigation extend the open exchange regions in permeable sediments. *Limnol. Oceanogr.* 52 (5), 1898–1909.
- Volkenborn, N., Polerecky, L., Wetthey, D.S., Woodin, S.A., 2010. Oscillatory pore-water bioadvection in marine sediments induced by hydraulic activities of *Arenicola marina*. *Limnol. Oceanogr.* 55, 1231–1247.
- Webb, A.P., Eyre, B.D., 2004. The effect of natural populations of the burrowing thalassinidean shrimp *Typaea australiensis* on sediment irrigation and benthic metabolism, nutrient fluxes and denitrification. *Mar. Ecol. Prog. Ser.* 268, 205–220.
- Wenzhöfer, F., Glud, R.N., 2004. Small-scale spatial and temporal variability in coastal benthic O<sub>2</sub> dynamics: effects of fauna activity. *Limnol. Oceanogr.* 49, 1471–1481.
- Werner, U., Bird, P., Wild, C., Ferdman, T., Polerecky, L., Eickert, G., Jonstone, R., Hoegh-Guldberg, O., de Beer, D., 2006. Spatial patterns of aerobic and anaerobic mineralization rates and oxygen penetration dynamics in coral reef sediments. *Mar. Ecol. Prog. Ser.* 309, 93–105.